

Fig. 4: Magnetic phase diagram of Gd<sub>6</sub>(Mn<sub>1-x</sub>Fe<sub>x</sub>)<sub>23</sub>. (a) Summary of element-specific  $T_{\rm C}$  values with XMCD and bulk magnetizations ( $M_{\rm Tot}^{\rm X}$  and  $M_{\rm Tot}^{\rm B}$ ) as a function of x. The plots of  $T_{\rm C(Gd)}$  (empty red circle O) and  $T_{\rm C(Fe)}$  (red cross circle ⊗) show three regions: (i) For 0.0 < x ≤ 0.15, bulk  $T_{\rm C}$  is determined by the Mn sublattice, and  $T_{\rm C(Gd)}$  = 273.5 K < bulk  $T_{\rm C}$ . (ii) For 0.15 < x ≤ 0.72, the Gd and Fe sublattices show the same  $T_{\rm C}$  = bulk  $T_{\rm C}$ . (iii) For 0.72 < x ≤ 1.0, the Fe moments determine the bulk  $T_{\rm C}$ , and  $T_{\rm C(Gd)}$  = 273.5 K < bulk  $T_{\rm C}$ . (b) Summary of Mn and Fe magnetic moments ( $\mu_{Mn}$ ,  $\mu_{Fe}$ ) as a function of x, showing switching of Mn moments for x ≥ 0.2 plotted with magnetic moments from 3s HAXPES analysis. [Reproduced from Ref. 1]

This report features the work of Ashish Chainani and his collaborators published in Commun. Mater. 5, 68 (2024) and Physical Review B 109, 035102 (2024).

## TLS 11A1 (Dragon) MCD, XAS SP 12U1 HAXPES/Photoemission

- XAS, XMCD, HAXPES
- Ferrimagnetic Transition, Materials Science, Condensed-matter Physics

#### References

- T. Ly Nguyen, T. Mazet, E. Gaudry, D. Malterre, F.-H. Chang, H.-J. Lin, C.-T. Chen, Y.-C. Tseng, A. Chainani, Commun. Mater. 5, 68 (2024).
- T. Ly Nguyen, T. Mazet, D. Malterre, H. J. Lin, M. Yoshimura, Y. F. Liao, H. Ishii, N. Hiraoka, Y. C. Tseng, A. Chainani, Phys. Rev. B 106, 045144 (2022).
- 3. A. Delapalme, J. Déportes, R. Lemaire, K. Hardman, W. J. James, J. Appl. Phys. **50**, 1987 (1979).
- 4. T. Ly Nguyen, C.-C. Yang, C.-H. Wang, Y.-W. Yang, T. Mazet, E. Gaudry, D. Malterre, M. Yoshimura, Y. F. Liao, H. Ishii, N. Hiraoka, H. J. Lin, Y. C. Tseng, A. Chainani, Phys. Rev. B **109**, 035102 (2024).

# **Unlocking Dual Topological States in the 2D Limit**

A promising way enhances the understanding of 2D topological materials and lays the groundwork for future electronic and superconducting applications.

Two-dimensional (2D) quantum materials have gained attention for their exceptional electronic properties, particularly in spintronics and quantum computing. Among them, 2D topological insulators (TIs) are notable for their protected metallic edge states, which exhibit spin-momentum locking and insusceptibility to backscattering from nonmagnetic impurities. These features make them strong candidates for low-power electronic devices and quantum computing. The discovery of topological nodal line semimetals (TNLSMs), which host one-dimensional nodal lines of band degeneracy in the Brillouin zone, has further expanded the landscape of topological materials. However, experimental realization of 2D TNLSMs remains rare despite numerous theoretical predictions. Stanene, the monolayer allotrope of tin (Sn), has emerged as a promising 2D TI because of its sizable topological band gap (~0.3 eV) induced by strong spin-orbit coupling (SOC). Unlike silicene and germanene, which possess much smaller SOC-induced gaps, stanene's robust band inversion enables the quantum spin Hall effect at room temperature. Additionally, stanene's electronic properties can be tuned *via* strain

engineering and substrate interactions, making it a versatile platform for investigating topological phase transitions. In contrast,  $\beta$ -Sn, a metallic allotrope of tin with a body-centered tetragonal structure, exhibits superconducting behavior and has potential applications in topological superconductivity. However, the electronic structure of ultrathin  $\beta$ -Sn films remains largely unexplored, leaving its potential as a 2D TNLSM unexamined.

To advance understanding of 2D TNLSMs, Pin-Jui Hsu and Horng-Tay Jeng, both from National Tsing Hua University, and Cheng-Maw Cheng from the NSRRC investigated the electronic structure of monolayer β-Sn grown on a Cu(111) substrate by using scanning tunneling microscopy (STM), angle-resolved photoemission spectroscopy (ARPES), and density functional theory (DFT) calculations. Their study probed the structural and electronic phase transition from honeycomb stanene (α-Sn) to cubic β-Sn as Sn coverage increased. The transition from a 2D TI to a 2D TNLSM was directly observed, revealing the coexistence of type-I and type-III nodal lines in monolayer  $\beta$ -Sn for the first time. Experimental observations aligned well with DFT calculations, confirming that  $\beta$ -Sn exhibits a nearly freestanding electronic structure on Cu(111), an unexpected behavior in a metal-on-metal system. This suggests that  $\beta$ -Sn/Cu(111) provides an ideal platform for studying intrinsic 2D TNLSM properties. Furthermore, integrating superconducting few-layer Sn with topological nodal line monolayer  $\beta$ -Sn could open new avenues for exploring 2D topological superconductivity and Majorana fermions. Comprehensive ARPES experiments at the **TLS 21B1** beamline were carried out on high-quality  $\alpha$ -Sn and  $\beta$ -Sn thin films prepared on Cu(111) using molecular beam epitaxy. A single layer of  $\alpha$ -Sn was first grown on a Cu(111) substrate at low temperature. STM and lowenergy electron diffraction revealed a honeycomb lattice of stanene with a  $p(2\times2)$  supercell. ARPES measurements confirmed the band structure's consistency with reported results. When an equivalent amount of Sn atoms was subsequently deposited onto the stanene/Cu(111) at low temperature, the honeycomb lattice disappeared, and a high-coverage Sn (HC-Sn) cubic  $\beta$ -Sn phase emerged, as observed in the STM images. This structural phase transition from semiconducting honeycomb  $\alpha$ -Sn to metallic cubic  $\beta$ -Sn provided a unique opportunity to investigate this topological transition in the band structure of ultrathin  $\beta$ -Sn(001) thin films.

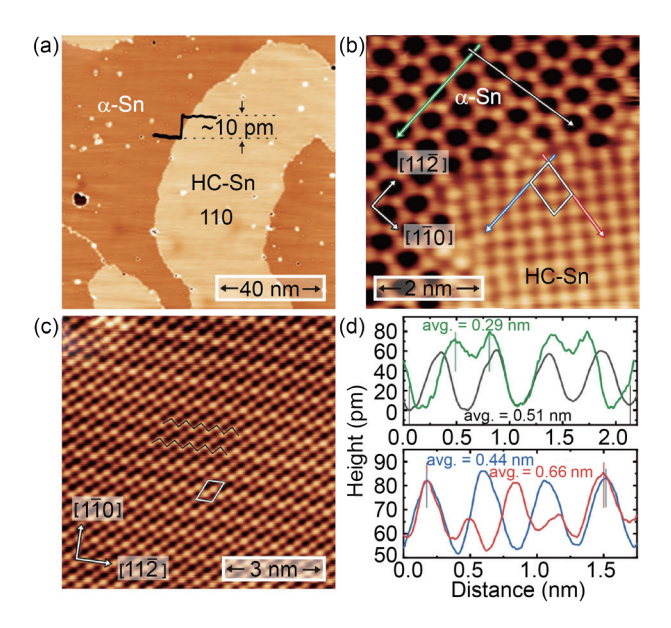


Fig. 1: (a) STM topographic overview of about 0.54 ML Sn grown on Cu(111). (b) Atomically resolved image at the boundary between α-Sn and HC-Sn. The white rhombuses indicate the unit cells of α-Sn ( $p(2\times2)$ ) and HC-Sn. (c) STM image of HC-Sn on a larger scan area with atomic resolution. The periodic zigzag pattern (black zigzag stripes) has been clearly resolved. White rhombus frame denotes the unit cell. (d) Top panel: black and green curves are topographic line profiles taken along the arrow lines on the α-Sn phase along [1  $\overline{1}$  0] and [1  $\overline{1}$   $\overline{2}$ ] directions, respectively, in (b). Bottom panel: topographic line profiles (red and blue curves) taken along the arrow lines on HC-Sn in (b). [Reproduced from Ref. 1]

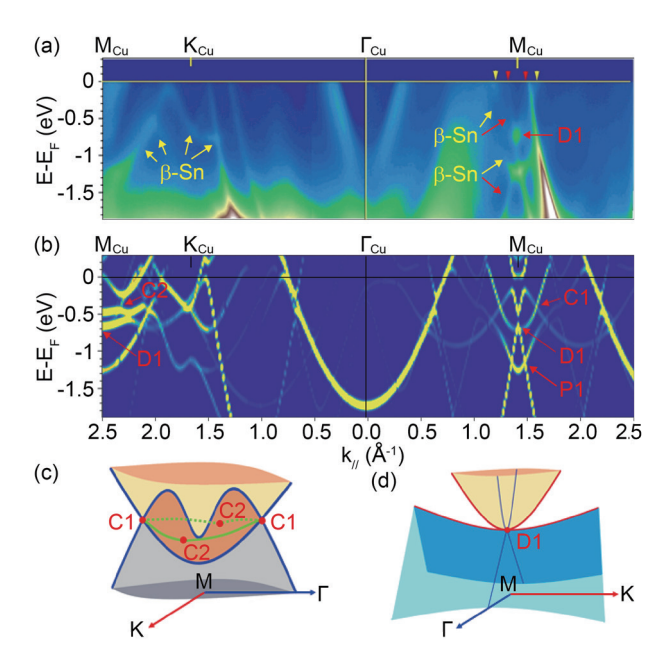


Fig. 2: (a) The band dispersions of single-layer β-Sn/Cu(111) along  $M_{\text{Cu}}\text{-}K_{\text{Cu}}\text{-}\Gamma_{\text{Cu}}\text{-}M_{\text{Cu}}$  relative to Cu(111) high-symmetry point direction. (b) The calculated unfolding band structure of freestanding monolayer β-Sn along the high symmetry lines in the BZ of Cu(111). Schematic diagram of type-I (c) and type-III (d) nodal line band crossings. C1 and C2 in (c) and D1 in (d) near the high-symmetry point  $M_{\text{Cu}}$  are indicated by the red arrows in (a) and (b). [Reproduced from Ref. 1]

STM topographic imaging of Sn thin films grown on Cu(111) at 80 K revealed distinct regions corresponding to α-Sn and β-Sn phases. We identified a honeycomb lattice with a  $p(2\times2)$  supercell in the darker regions characteristic of α-Sn, while the brighter regions exhibited a higher-coverage Sn phase with a denser atomic arrangement. DFT calculations confirmed that the interlayer distance between the top  $\beta$ -Sn layer and the first Cu layer was 2.40 Å, consistent with the STM findings. To explore evolution in electronic structure from low-coverage (LC) to high-coverage (HC) Sn phases on Cu(111), ARPES measurements were conducted. Relative to pristine Cu(111), a linear band dispersion with a Dirac point at 0.62 eV binding energy emerged around the  $M_{Cu}$  point for  $\beta$ -Sn/Cu(111) shown in **Fig. 2(a)**, indicating an electronic topological transition. Two wave vectors crossing the Fermi level were identified, along with two electron pockets around the M<sub>Cu</sub> point: one with significant Fermi level crossing and another deeper in the binding energy region. Additional β-Sn-derived bands, which are confirmed as 2D features through photon energy-dependent ARPES experiments, appeared at the  $K_{Cu}$  point. DFT band structure calculations were performed for both freestanding monolayer  $\beta$ -Sn and  $\beta$ -Sn/Cu(111). The unfolded band structure of freestanding  $\beta$ -Sn monolayer closely matched ARPES results, particularly around the  $M_{Cu}$  and  $K_{Cu}$  points. The bandcrossing points C1 and D1 near M<sub>Cu</sub> were identified as type-I and type-III nodal line semimetal features. The C1 crossing formed a closed ring-shaped type-I nodal line, while the D1 crossing exhibited a type-III nodal line characterized by a conesaddle intersection. These findings confirm that  $\beta$ -Sn/Cu(111) hosts a dual-nodal line semimetal phase, making it an exciting candidate for further exploration of 2D TNLSMs.

Similar to reported 2D nodal line materials such as CuSe, AgSe, and  $Cu_2Si$ , monolayer  $\beta$ -Sn possesses mirror reflection symmetry. In three-dimensional TNLSMs, nodal line projections onto surfaces generate drumhead-like flat surface bands protected by topological invariants. However, in 2D TNLSMs, node lines do not directly protect edge states, complicating their observation. Despite this challenge,  $\beta$ -Sn's coexistence of type-I and type-III nodal lines presents an exceptional case for further research. Few experimental realizations of 2D TNLSMs exist due to stringent symmetry and SOC requirements. While theoretical predictions suggest that external perturbations like strain or electric fields can induce a TNLSM phase in some 2D materials, experimental verification remains scarce. The discovery of type-I and type-III gapless nodal line behaviors in  $\beta$ -Sn/Cu(111) marks a significant step forward. These findings, backed by STM-ARPES-DFT investigations, establish monolayer  $\beta$ -Sn as a novel 2D dual-nodal line semimetal, offering a valuable platform for exploring topological superconductivity and other quantum phenomena.

To summarize, by elucidating topological transition and nodal line behavior in ultrathin  $\beta$ -Sn films, this work enhances the understanding of 2D topological materials and lays the groundwork for future electronic and superconducting applications. The unique properties of  $\beta$ -Sn highlight its potential as a novel material for next-generation quantum devices. (Reported by Cheng-Maw Cheng)

This report features the work of Pin-Jui Hsu, Horng-Tay Jeng, Cheng-Maw Cheng and their collaborators published in ACS Nano 18, 20990 (2024).

### TLS 21B1 Angle-resolved UPS

- High-resolution ARPES
- Materials Science, Condensed-matter Physics

### Reference

1. Y.-S. Lan, C.-J. Chen, S.-H. Kuo, Y.-H. Lin, A. Huang, J.-Y. Huang, P.-J. Hsu, C.-M. Cheng, H.-T. Jeng, ACS Nano 18, 20990 (2024).